MISSOURI S&T

Missouri University of Science and Technology

Scholars' Mine

International Specialty Conference on Cold-Formed Steel Structures

(1994) - 12th International Specialty Conference on Cold-Formed Steel Structures

Oct 18th, 12:00 AM

Comparison of a Non-linear Purlin Model with Tests

Catherine J. Rousch

Gregory J. Hancock

Follow this and additional works at: https://scholarsmine.mst.edu/isccss

Part of the Structural Engineering Commons

COMPARISON OF A NON-LINEAR PURLIN MODEL WITH TESTS

C.J. Rousch [*]   G.J. Hancock [†]

SUMMARY

A non-linear elastic analysis has been developed for determining the lateral deflections of, and stresses in, the unconnected flanges of simply-supported and continuous channel and Z-section purlins screw-fastened to sheeting and subject to either wind uplift or gravity loading. The analysis incorporates a model, based on a combination of those developed by Peköz and Soroushian, and Thomasson, which depicts the unconnected purlin flange as a beam-column. The restraint against lateral deflection is provided primarily by the sheeting, and is represented by a linear extensional spring of stiffness k located at the level of the unconnected purlin flange.

To verify the model, lateral deflections and failure stresses obtained from vacuum rig tests can be compared with those determined by the non-linear analysis. In this paper, results from vacuum rig tests on continuous Z-section purlins screw-fastened to sheeting and subject to simulated wind uplift and gravity loading are compared.

1   INTRODUCTION

Roof systems commonly used throughout the world often consist of cold-formed steel channel or Z-section purlins fastened to high tensile profiled steel sheeting. Two major problem areas are encountered in the design of cold-formed steel purlins. Firstly, the sections are generally not doubly-symmetric as for conventional beam design, and secondly, the magnitude of restraint provided by sheeting, bridging (bracing) and cleats is difficult to quantify. Cold-formed steel purlins tend to be efficient, however, as the restraint provided by the sheeting, bridging and cleats tends to adequately counteract the adverse effect of using mono-symmetric and point-symmetric sections. It is the lack of data available on these counteracting effects which produces the uncertainty.

Despite their widespread use, very little data regarding the buckling failure modes, stresses and deflections of these roof systems is available. The purpose of this paper is to provide and verify a model, based on a combination of those developed by Peköz and Soroushian (1982), and Thomasson (1988), which can be used to calculate the lateral deflections of, and stresses in, the unconnected flanges of both simply-supported and continuous cold-formed steel channel and Z-section purlins screw-fastened to sheeting and subject to either wind uplift or gravity loading.

---

[*]PhD Research Student, School of Civil and Mining Engineering, University of Sydney NSW 2006 Australia
[†]Professor, School of Civil and Mining Engineering, University of Sydney NSW 2006 Australia

This model has been incorporated in a second order (non-linear) elastic analysis, developed at the University of Sydney. In this paper, lateral deflections and stresses obtained from the analysis are compared with those determined experimentally for a continuous lapped Z-section purlin screw-fastened to sheeting and subject to simulated wind uplift and gravity loading.

2 DESIGN MODELS

2.1 General

Two fundamentally different models of the buckling modes of cold-formed steel channel and Z-section purlins have been developed. These are the distorted section model, or D model, and the undistorted section model, or U model. The U model is based on the thin-walled beam theories of Timoshenko (1961) and Vlasov (1961), in which stability can be computed using the conventional stability theory of thin-walled beams with undistorted cross-sections. The D model has required the development of a new stability model to account for section distortion, which is not considered in the Timoshenko and Vlasov theories. In the D model, the unconnected purlin flange will become unstable under wind uplift or gravity loading if the lateral restraint provided through the web is insufficient in preventing column buckling of that flange. The D and U section models for purlins under wind uplift are shown in Fig. 1a for a Z-section and in Fig. 1b for a channel.

There are two different types of purlin-sheeting connections commonly used in practice. The first is a screw-fastened system in which the sheeting is screw-fastened to the purlin through its troughs (pans) or crests using self-tapping screws. Screw-fastened systems are commonly used throughout the world, and usually provide adequate transfer of both lateral and torsional restraint from the sheeting to the purlin. For this reason, the D model is deemed the most appropriate stability model for screw-fastened systems. The second type involves the use of clips or concealed fasteners, usually with standing seam roofs or interlocking sheeting. This roof system provides very little lateral or torsional restraint to the purlin, and hence the U model, in which the sheeting is assumed to provide no torsional restraint to the attached purlin, may be the more appropriate stability model in this case.

2.2 Distorted Section Model

If a wind uplift or gravity load is applied parallel to a purlin section web, and there is no lateral or torsional restraint provided by sheeting, then a Z-section will move vertically and deflect laterally as a result of its inclined principal axes, and a channel will move vertically and twist as a result of the eccentricity of the applied load from its shear centre. However, if adequate lateral restraint and some degree of torsional restraint is applied, both Z-sections and channels will undergo vertical deflection and twisting, including section distortion. Peköz and Soroushian proposed that these deformations occur in two stages; the vertical bending stage, and the torsion stage, as depicted in Fig. 2a for a channel under wind uplift.

The vertical bending stage can be analysed using simple flexure theory. The torsion stage can be analysed by modelling the unconnected purlin flange and a section of the web as a beam-column on an elastic foundation. The stiffness of this foundation is determined by idealising the purlin-sheeting connection as a rotational spring, located at the centre of purlin rotation. (Purlin rotation is at the junction of the web and the connected flange for a Z-section, and at

the purlin-sheeting connection for a channel.) The rotational spring is then converted to a linear extensional spring of stiffness k located at the level of the unconnected purlin flange, as shown in Fig. 2b. This linear extensional spring consists of the flexural stiffness of the sheeting combined with the flexural stiffness of the purlin web and the rotational stiffness of the purlin-sheeting connection, and thus restrains the unconnected purlin flange against lateral deflection.

When a uniformly distributed wind uplift or gravity load, q, is applied parallel to the purlin web, a uniformly distributed lateral load, w, is induced in the unconnected flange. Peköz and Soroushian calculated the lateral load induced in the unconnected flange of a simply-supported channel or Z-section purlin under wind uplift as being equal to

$$w = q(\frac{Qb}{2I} + \alpha) \tag{1}$$

where Q is the moment of the beam-column section about the purlin centroidal axis perpendicular to the web, b is the total width of the unconnected purlin flange, I is the second moment of area of the effective deflected purlin section about the centroidal axis perpendicular to the undeflected position of the web, and α is the distance from the centre of purlin rotation to the flange-web junction divided by the web depth, H. For a Z-section, α is therefore equal to zero, and Eq. 1 becomes

$$w = q(\frac{Qb}{2I}) \tag{2}$$

Peköz and Soroushian suggested that Q could be simplified by ignoring the contribution of both the web and the lip to the beam-column section so that

$$Q = \frac{btH}{2} \tag{3}$$

where t is the thickness of the purlin section.

Rousch, Rasmussen and Hancock (1993) proved that Eq. 2 is valid for both simply-supported *and* continuous Z-section *and* channel purlins under wind uplift, as the lateral load, w, induced in the unconnected flange of a channel is the same as that induced in the unconnected flange of its equivalent Z-section. (Full details of this proof can be found in Appendix A of Rousch and Hancock (1994).) This conclusion may be specific to Australian purlin-sheeting systems where channels and Z-sections appear to be equally restrained from twisting. Peköz and Soroushian do not report the relative magnitudes of twisting of these sections.

Like Peköz and Soroushian, Thomasson also developed the idea of modelling the unconnected purlin flange and a section of the web as a beam-column on an elastic foundation. He applied this concept when modelling the distortion of both simply-supported and continuous Z-section purlins. Thomasson included both the lip and a certain part of the web, x, in the beam-column calculations, and suggested that two different beam-column sections be used; one with x equal to x_1, as shown in Fig. 3a, to obtain the correct lateral deflections of the unconnected flange, and one with x equal to x_2, as shown in Fig. 3b, to obtain the correct values of stress distribution in the unconnected flange. However for practical purposes, Thomasson thought it reasonable to set a fixed value of x valid for both x_1 and x_2. The Swedish Code for Light-Gauge Steel Members (1982) sets x equal to 27 percent of the total web depth. For Australian made Z-sections and

channels, x should be taken as being equal to 35.5 percent of the total web depth. The details of Thomasson's model can be found in Appendix B of Rousch and Hancock.

The second order (non-linear) elastic analysis model presented in this paper requires calculation of the lateral load, w, induced in the unconnected flange of a simply-supported or continuous channel or Z-section purlin when a wind uplift or gravity load is applied parallel to the section web, using Eq. 2 provided by Peköz and Soroushian. Both the lip and a section of the web, x, as suggested by Thomasson, should be included in the calculation of the beam-column moment, Q.

3 SECOND ORDER (NON-LINEAR) ELASTIC ANALYSIS

3.1 General

Second order (non-linear) elastic analysis is a method used for determining the stresses and elastic deformations of structures whilst accounting for changes in geometry. The deformations are usually small but finite, hence the term *second order*, and the equations developed for their solution are *non-linear* in the deformations. The equations can be solved using iterative techniques as described by Hancock (1991). A second order elastic analysis has been developed for the specific purpose of determining the lateral deflections of, and stresses in, the unconnected flanges of simply-supported and continuous channel and Z-section purlins under either wind uplift or gravity loading. This analysis includes the effects of continuous restraint.

A typical continuous purlin-sheeting system with a uniformly distributed uplift load, q, applied parallel to the purlin web is depicted in Fig. 4a. The cross-sectional area, A, and second moment of area, I, are assumed to be doubled at the lapped sections. Initially, a first order (linear) elastic analysis for bending in the plane of the web is performed on the purlin to calculate its vertical deflection and bending moment distribution. The axial compressive force distribution, p, induced in the unconnected flange by the in-plane bending, is determined from the results of the in-plane analysis. A second order (non-linear) elastic analysis is then performed to determine the lateral deflection of the unconnected purlin flange. This flange is idealised by the Peköz and Soroushian beam-column model, and includes both the lip and a section of the web, x, as suggested by Thomasson. The beam-column section, including the axial compressive force, p, resulting from the first order analysis, the induced uniformly distributed lateral load, w, given by Eq. 2, and the lateral restraint of stiffness k, is shown in Fig. 4b.

3.2 Second Order Element Stiffness Matrix

The unconnected purlin flange can be divided along its span into elements of length L. A 6 × 6 second order element stiffness matrix, $[k_m^*]$, can be formed for each element. The stiffness matrix, in local x-y axes, relates the forces, $\{F_m\}$, to the joint displacements, $\{x_m\}$, such that

$$\{F_m\} = [k_m^*]\{x_m\} \tag{4}$$

where

$$\{F_m\} = \left\{ \begin{matrix} F_{xA} & F_{yA} & M_{AB} & F_{xB} & F_{yB} & M_{BA} \end{matrix} \right\}^T$$

and

$$\{x_m\} = \left\{ \begin{matrix} x_A & y_A & \theta_{AB} & x_B & y_B & \theta_{BA} \end{matrix} \right\}^T$$

Both forces and displacements are aligned with the initial member position as shown in Fig. 5..If the deflected shape of the element is assumed to be a cubic polynomial, then $[k_m^*]$ can be linearised in the axial load, p, such that it is given by the sum of the linear elastic, $[k_m]$, and geometric, $[g_m]$, element stiffness matrices as shown by Rubinstein (1970):

$$[k_m^*] = [k_m] + p \cdot [g_m] \tag{5}$$

where

$$[k_m] = \begin{bmatrix} \frac{EA}{L} & 0 & 0 & -\frac{EA}{L} & 0 & 0 \\ 0 & \frac{12EI}{L^3} & -\frac{6EI}{L^2} & 0 & -\frac{12EI}{L^3} & -\frac{6EI}{L^2} \\ 0 & -\frac{6EI}{L^2} & \frac{4EI}{L} & 0 & \frac{6EI}{L^2} & \frac{2EI}{L} \\ -\frac{EA}{L} & 0 & 0 & \frac{EA}{L} & 0 & 0 \\ 0 & -\frac{12EI}{L^3} & \frac{6EI}{L^2} & 0 & \frac{12EI}{L^3} & \frac{6EI}{L^2} \\ 0 & -\frac{6EI}{L^2} & \frac{2EI}{L} & 0 & \frac{6EI}{L^2} & \frac{4EI}{L} \end{bmatrix}$$

and

$$[g_m] = \begin{bmatrix} 0 & 0 & 0 & 0 & 0 & 0 \\ 0 & -\frac{6}{5L} & \frac{1}{10} & 0 & \frac{6}{5L} & \frac{1}{10} \\ 0 & \frac{1}{10} & -\frac{4L}{30} & 0 & -\frac{1}{10} & \frac{L}{30} \\ 0 & 0 & 0 & 0 & 0 & 0 \\ 0 & \frac{6}{5L} & -\frac{1}{10} & 0 & -\frac{6}{5L} & -\frac{1}{10} \\ 0 & \frac{1}{10} & \frac{L}{30} & 0 & -\frac{1}{10} & -\frac{4L}{30} \end{bmatrix}$$

3.3 Element Restraint Matrix

By assuming that the deflection of each element is in the shape of a cubic polynomial, an element restraint matrix, $[r_m]$, can be determined. (The derivation of the restraint matrix is given in Appendix C of Rousch and Hancock.) The restraint matrix represents the lateral restraint of stiffness k in the Peköz and Soroushian beam-column model. The 6×6 element restraint matrix is

$$[r_m] = \frac{kL}{420} \begin{bmatrix} 0 & 0 & 0 & 0 & 0 & 0 \\ 0 & 156 & -22L & 0 & 54 & 13L \\ 0 & -22L & 4L^2 & 0 & -13L & -3L^2 \\ 0 & 0 & 0 & 0 & 0 & 0 \\ 0 & 54 & -13L & 0 & 156 & 22L \\ 0 & 13L & -3L^2 & 0 & 22L & 4L^2 \end{bmatrix}$$

The element restraint matrix, $[r_m]$, can be added to the second order element stiffness matrix, $[k_m^*]$, so that Eq. 4 becomes

$$\{F_m\} = ([k_m^*] + [r_m])\{x_m\} \tag{6}$$

The lateral deflection of the unconnected purlin flange can now be solved using the iterative techniques mentioned earlier.

3.4   Verification of Model

The use of a restraint matrix, $[r_m]$, to represent the lateral restraint of stiffness k in the Peköz and Soroushian model can be verified using equations proposed by Timoshenko and Gere (1961) for the buckling of a beam on an elastic foundation. The lateral deflections obtained from the second order analysis incorporating the restraint matrix can be compared with those found using equations proposed by Hetényi (1971) for the deflection of a beam on an elastic foundation.

3.4.1   Buckling of a Beam on an Elastic Foundation

A plane rigid frame buckling analysis developed at the University of Sydney can be used to perform frame buckling analyses using linear eigenvalue routines. The buckling modes and loads of a beam with lateral restraint can be determined by adding the restraint matrix to the linear elastic stiffness matrix such that the resulting eigenvalue problem is

$$([K] + [R])\{X\} - \lambda[G]\{X\} = \{0\} \tag{7}$$

where $[K]$ is the linear elastic global stiffness matrix assembled from the individual $[k_m]$ element stiffness matrices, $[R]$ is the global restraint matrix assembled from the individual $[r_m]$ element restraint matrices, $[G]$ is the geometric global stiffness matrix assembled from the individual $[g_m]$ geometric element stiffness matrices, λ is the load factor and $\{X\}$ is the vector of joint displacements in global X-Y axes. The buckling load, P_b, of a simply-supported beam with lateral restraint of stiffness k can therefore be obtained by solving Eq. 7 using the buckling analysis.

P_b can be compared with the critical buckling load, P_{cr}, obtained from equations derived by Timoshenko and Gere (outlined in Appendix D of Rousch and Hancock) for the buckling of a simply-supported beam on a continuous elastic foundation of stiffness k. P_b and P_{cr} are compared here for a simply-supported 7.0m (23.0 ft) span beam on a continuous elastic foundation of stiffness k. The beam had a second moment of area, I, and cross-sectional area, A, equal to 6.012E+6mm^4 (14.4in.^{4}) and 934.092mm^2 (1.4in.^{2}) respectively. (These values are typical of those of a *Lytgal* Z20024 Z-section purlin.) Table 1 compares the results when an axial compressive load, P, equal to 1000 N (225 lb), was applied at either end of the purlin as shown in Fig. 6a. P_b and P_{cr} are found to compare favourably. The buckling analysis also showed that the beam buckled in a single half-wave for all values of k less than 0.196 N/mm^2 (28.4 lb/in.^{2}). This buckling mode was affirmed for all values of k less than 0.195 N/mm^2 (28.3 lb/in.^{2}) using the Timoshenko and Gere equations. Table 2 compares the results when a *distributed* axial compressive load, p, was applied as shown in Fig. 6b. The distributed loading used to find P_b

was that induced in the beam when a uniformly distributed uplift load of 1 N/mm (5.7 lb/in.) was applied. Again, P_b and P_{cr} are found to compare favourably.

3.4.2 Deflection of a Beam on an Elastic Foundation

The second order elastic analysis was used to determine the midspan deflection of a simply-supported 5.0m (16.4 ft) span beam on a continuous elastic foundation of stiffness k when a uniformly distributed gravity load, q, equal to 1 N/mm (5.7 lb/in.), was applied as shown in Fig. 7a. The beam had a second moment of area, I, equal to 1.0E+8mm^4 (240.3in.^{4}), and a cross-sectional area, A, of 1.0E+5mm^2 (155.0in.^{2}). Table 3 compares the deflection, y, found at the midspan using the analysis, with the deflection, y_H, calculated at the midspan using Hetényi's equation for a beam on an elastic foundation of modulus k. The beam was re-analysed with the addition of an axial compressive load, P, equal to 10000 N (2.2 kip), applied at either of its ends as shown in Fig. 7b. The deflections at the midspan are compared in Table 4. For both load cases, the midspan deflections obtained using the analysis compare favourably with those calculated using Hetényi's equations. Details of Hetényi's equations can be found in Appendix D of Rousch and Hancock.

4 STRESS CALCULATIONS

From the bending moments determined in the first order (linear) and the second order (non-linear) analyses discussed in Section 3, stress distributions in the connected and unconnected purlin flanges of a simply-supported or continuous channel or Z-section purlin may be calculated. If the distribution of stresses along the length of a purlin is known, then the failure criteria, including the mode of failure, may be determined.

4.1 Combining Stresses

The stress, σ_x, in the purlin flange (at any given point along the purlin span) resulting from in-plane bending only is given by the equation

$$\sigma_x = \frac{M_x \cdot y}{I_{xeff}} \tag{8}$$

where M_x is the in-plane bending moment, y is the (vertical) distance from the centroid of the effective purlin section to the extreme outer fibre of either the connected or unconnected purlin flanges, and I_{xeff} is the second moment of area of the effective deflected purlin section about the centroidal axis perpendicular to the undeflected position of the web. As a result of lateral deflection and twist, the second moment of area, I_{xeff}, is reduced, and is therefore given by the equation

$$I_{xeff} = I_{x0}[1 - (\frac{a_1}{H})^2] \tag{9}$$

where I_{x0} is the second moment of area of the effective undeflected purlin section about the

centroidal axis perpendicular to the web, H is the purlin web depth and a_1 is the lateral deflection of the unconnected purlin flange as determined by the second order analysis.

The out-of-plane stresses, σ_y, are only calculated in the unconnected purlin flange, and may be determined from the equation

$$\sigma_y = \frac{M_y \cdot x}{I_f} \qquad (10)$$

where, at any point along the purlin span, M_y is the out-of-plane bending moment, I_f is the second moment of area of the beam-column section (comprising the unconnected purlin flange, lip and percentage of the web) about its centroidal axis parallel with the purlin web, and x is the (horizontal) distance from the centroid of the beam-column section to the point along the unconnected flange at which the stress is required (usually at the flange-web or flange-lip junction).

The total stress in the connected purlin flange at any point along the purlin span is equal to the stress resulting only from in-plane bending, and is therefore given by Eq. 8. The total stress distribution in the unconnected flange is equal to the addition of the stresses resulting from both in-plane and out-of-plane bending, and is therefore given by the sum of Eq. 8 and Eq. 10.

4.2 Failure Criteria

Vacuum rig tests simulating wind uplift and gravity loading on simply-supported and continuous cold-formed steel channel and Z-section purlins screw-fastened to roof sheeting have been performed at the Centre for Advanced Structural Engineering (1989, 1990a) within the University of Sydney, and the test results have been published in Hancock, Celeban and Healy (1993). These tests showed that the mode of failure varied for purlins with and without bridging. Under wind uplift, continuous Z-section and simply-supported Z-section and channel purlins without bridging were all found to fail by local buckling at the flange-web junction of the unconnected purlin flange. For purlins with one or more rows of bridging in each span, failure was by flange-web buckling, lip stiffener buckling or general flange failure. When subject to gravity loading, continuous Z-section purlins both with and without bridging failed initially by flange-web local buckling. For purlins with cleat supports, subsequent loading generally resulted in lip stiffener buckling and general flange failure. For purlins without cleat supports, substantial lateral bending of the cleats occurred.

The failure stress at the flange-web junction can be determined from the equations in the AISI Specification (1980) and in the Australian Cold-Formed Steel Structures Code (1988) with the factor of safety removed. The limiting stress, F_{bw}, at the flange-web junction is therefore given by the equation

$$F_{bw} = [1.21 - 0.00013(\frac{d_1}{t})\sqrt{F_y}] \, F_y \qquad (11)$$

where d_1 is the clear distance between the flanges, t is the nominal steel thickness exclusive of coatings, and F_y is the yield stress of the steel.

5 CONTINUOUS PURLIN EXAMPLE

5.1 Wind Uplift Loading

A three span continuous lapped *Lytgal* Z20015 Z-section screw-fastened to roof sheeting and subject to wind uplift is shown in Fig. 8. This system corresponds with that of the Series 1 Test 4(A) vacuum rig test performed at the University of Sydney (Hancock, Celeban and Healy) in which four equally spaced three span continuous Z20015 purlins screw-fastened to sheeting were subject to a simulated wind uplift loading. The lateral deflections of the unconnected flanges of the two inner purlins were measured with each increment in loading. The deflections were measured at the midpoint of the end spans using displacement transducer gauges, labelled G3 and G5 at the northern end, and G15 and G17 at the southern end, as shown in Fig. 9. Standard two-hole cleats were used. Loading was increased from zero load until failure of one of the purlins was obtained. Failure occurred when a uniform line load of approximately 2.58 N/mm (14.7 lb/in.), corresponding to 2.0 kPa (0.3 psi) pressure in the rig, was applied on the inner purlins.

The second order elastic analysis can be used to predict the lateral displacement of the unconnected purlin flange at any given load if the value of restraint, k, provided by the sheeting to the purlin is known. Purlin-sheeting connection tests were carried out at the Centre for Advanced Structural Engineering (1990b) within the University of Sydney to determine the values of restraint for channel and Z-section purlins of various sizes screw-fastened to sheeting. For a Z20015, k was found to be approximately 0.018 N/mm² (2.6 lb/in.²). Fig. 10 compares the lateral displacements of the unconnected purlin flange at the midpoint of the end spans as determined by the analysis with k equal to 0.018 N/mm² (2.6 lb/in.²), with those determined in the vacuum rig test.

By using the bending moment distributions obtained from the analysis with k equal to 0.018 N/mm² (2.6 lb/in.²), a stress analysis was performed at the failure load. From this analysis it was found that the maximum compressive stress occurred at the flange-web junction of the unconnected purlin flange at a position just to one side of the midpoint of the end spans, as shown in Fig. 9. The stress distributions in the flanges at this point are given in Fig. 11a. Hence flange-web buckling, occurring at a position near the midpoint of the end spans, was the predicted failure mode. The vacuum rig test did in fact fail by flange-web buckling near the midpoint of the northern end spans of the two inner purlins. The maximum compressive stress in the connected purlin flange occurred adjacent to the lapped joints on the inner span, shown also in Fig. 9. The stress distributions in the flanges at this point are given in Fig. 11b. The failure stress, F_{bw}, at the flange-web junction can be computed using Eq. 11 with $F_y = 520$ MPa (75.4 ksi), $d_1 = 198.98$mm (7.8in.) and $t = 1.46$mm (0.06in.). The resulting stress of 419 MPa (60.8 ksi) compares closely with the theoretical value of 413 MPa (59.9 ksi) obtained from the stress analysis at the failure load.

5.2 Gravity Loading

The Series 4 Test 4 vacuum rig test performed at the University of Sydney (Hancock, Celeban and Healy) consisted of four equally spaced three span continuous lapped *Lytgal* Z20015 purlins screw-fastened to sheeting as in Series 1 Test 4(A), but subject to a simulated gravity loading. The lateral deflections were measured at the midpoint of the end spans using displacement transducer gauges G3 and G5 at the northern end, and G15 and G17 at the southern end as shown

in Fig. 12. To prevent lateral deformation of the cleats, cleat supports were provided. Failure occurred when a uniform line load of approximately 2.94 N/mm (16.8 lb/in.), corresponding to 2.43 kPa (0.4 psi) pressure in the rig, was applied on the inner purlins. Fig. 13 compares the lateral displacements of the unconnected purlin flange at the midpoint of the end spans as determined by the analysis with $k = 0.018$ N/mm^2 (2.6 lb/in.^{2}), with those determined in the vacuum rig test. The theoretical deflection is close to linear. The experimental values indicate a stiffening of the restraint. It is presumed that under gravity loading, the sheeting bears against the purlin and increases the k value. Further experimental research on this phenomenon is required.

A stress analysis at the failure load found that the maximum compressive stress occurred at the flange-web junction of the unconnected purlin flange at a location adjacent to the lapped joints on the inner span, as shown in Fig. 12. The stress distributions in the flanges at this point are shown in Fig. 14a. This flange-web buckling failure mode, occurring adjacent to the lapped joints on the inner span, corresponds with the vacuum rig test flange-web buckling failures at the same positions. The maximum compressive stress in the connected purlin flange occurred just to one side of the midpoint of the end spans, shown also in Fig. 12. The stress distributions in the flanges at this point are shown in Fig. 14b. The failure stress, F_{bw}, at the flange-web junction computed using Eq. 11 with $F_y = 520$ MPa (75.4 ksi), $d_1 = 199.96$mm (7.6in.) and t = 1.47mm (0.06in.), resulted in a stress of 420 MPa (60.9 ksi). This lies within 4 percent of the theoretical value of 437 MPa (63.4 ksi) obtained from the stress analysis at the failure load. The analysis values are slightly higher than those calculated using Eq. 11 as a result of the greater theoretical lateral deflection of the unrestrained flange than observed experimentally.

6 CONCLUSION

A second order (non-linear) elastic analysis has been developed for determining the lateral deflections of, and stresses in, the unconnected flanges of simply-supported and continuous channel and Z-section purlins screw-fastened to sheeting and subject to either wind uplift or gravity loading. The restraint provided by the sheeting against lateral deflection of the unconnected purlin flange is represented by a linear extensional spring of stiffness k located at the level of the unconnected purlin flange, which is modelled as a beam-column. The value of k can be incorporated in a restraint matrix which is added to the second order stiffness matrix of the beam-column, and the lateral deflection of the unconnected purlin flange can then be solved for using iterative techniques. Stresses are computed assuming bending in the plane of the web (using the properties of the effective section) and lateral deflection of the beam-column. The model is similar to that proposed by Peköz and Soroushian for simply-supported purlins, but is extended to continuous purlin systems, with a beam-column element of the type proposed by Thomasson, in which both the flange lip and percentage of the web are included.

A three span continuous Z-section purlin screw-fastened to sheeting was used to demonstrate the applicability of the model. The lateral deflections and failure stresses obtained from the second order analysis were found to compare favourably with those determined experimentally for both wind uplift and gravity loading. In the case of gravity loading, the stiffening of the restraint provided by the sheeting under increased load requires further experimental investigation.

7   ACKNOWLEDGEMENTS

APPENDIX A. REFERENCES

American Iron and Steel Institute (1980), *Specification for the Design of Cold-Formed Steel Structural Members*, Washington D.C., U.S.A.

Centre for Advanced Structural Engineering, "Vacuum Test Rig Common Purlin Test Program Series 1, 2, 3 & 4", Research Reports S754 (1989), S761 (1990), S768 (1990), S819 (1990), School of Civil and Mining Engineering, The University of Sydney, Australia.

Centre for Advanced Structural Engineering, "Vacuum Test Rig Common Purlin Test Program Series 1, 2 & 3, Sheeting/Purlin Connection Tests", Research Report S786 (1990), School of Civil and Mining Engineering, The University of Sydney, Australia.

Hancock, G.J. (1991), "Second Order Elastic Analyses Solution Techniques and Verification", Lecture Notes, *Structural Analysis to AS4100* Postgraduate Course, School of Civil and Mining Engineering, The University of Sydney, Australia.

Hancock, G., Celeban, M. and Healy, C. (1993), "Behaviour of Purlins with Screw Fastened Sheeting under Wind Uplift and Downwards Loading", *Australian Civil Engineering Transactions*, Vol. CE35 No. 3, pp 221-233.

Hetényi, M. (1971), "Beams on Elastic Foundation - Theory with Applications in the Fields of Civil and Mechanical Engineering", The University of Michigan Press, Ann Arbour, Michigan, U.S.A.

Peköz, T. and Soroushian, P. (1982), "Behaviour of C- and Z- Purlins Under Wind Uplift", *6th Specialty Conference on Cold-Formed Steel Structures*, pp 409-429, University of Missouri-Rolla, St Louis, Missouri, U.S.A.

Rousch, C.J. and Hancock, G.J. (1994), "A Non-Linear Model for Simply-Supported and Continuous Purlins", Research Report R688, School of Civil and Mining Engineering, The University of Sydney, Australia.

Rousch, C.J., Rasmussen, K.J.R. and Hancock, G.J. (1993), "Bending Strengths of Cold-Formed Channel and Z Sections Restrained by Sheeting", *International Workshop on Cold-Formed Steel Structures*, Sydney, Australia.

Rubinstein, M.F. (1970), "Structural Systems - Statics, Dynamics and Stability", Prentice-Hall, Inc., Englewood Cliffs, New Jersey, U.S.A.

Standards Association of Australia, AS1538 (1988), *Cold-Formed Steel Structures Code*, North Sydney, Australia.

Swedish Institute of Steel Construction (1982), *Swedish Code for Light-Gauge Metal Structures*, Publication 76.

Thomasson, P.O. (1988), "On the Behaviour of Cold-Formed Steel Purlins - Particularly with Respect to Cross Sectional Distortion", Baehre-Festschrift, pp 281-292.

Timoshenko, S.P. and Gere, J.M. (1961), "Theory of Elastic Stability", 2nd Edition, McGraw-Hill, New York, New York, U.S.A.

Vlasov, V.Z. (1961), "Thin-walled Elastic Beams", 2nd Edition, Israel Program for Scientific Translations, Jerusalem.

APPENDIX B. NOTATION

a_1	lateral deflection of unconnected purlin flange
A	cross-sectional area of effective purlin section
A_f	cross-sectional area of beam-column section
b	width of unconnected purlin flange
d_1	clear distance between flanges
F_{xA}, F_{yA}, M_{AB}	forces and moment in local x-y axes
F_{bw}	limiting stress at flange-web junction
F_y	yield stress
H	purlin web depth
I, I_{xeff}	second moment of area of the effective deflected purlin section about the centroidal axis perpendicular to the undeflected position of the web
I_f	second moment of area of beam-column section about its centroidal axis parallel with the purlin web
I_{x0}	second moment of area of the effective undeflected purlin section about the centroidal axis perpendicular to the web
k	stiffness of lateral restraint
l	length of span
L	length of element
M_x	in-plane bending moment
M_y	out-of-plane bending moment
p	distributed axial compressive force induced in unconnected purlin flange *or* applied distributed axial compressive load
P	applied axial compressive load
P_b	buckling load
P_{cr}	critical buckling load
q	uniformly distributed wind uplift or gravity load applied parallel to purlin web
Q	moment of beam-column section about purlin centroidal axis perpendicular to web
t	purlin thickness *or* nominal steel thickness exclusive of coatings
w	uniformly distributed lateral load induced in unconnected purlin flange

x	horizontal distance from beam-column centroid
	or depth of purlin web included in beam-column section
x_1	depth of purlin web included in beam-column section to obtain correct lateral deflection of unconnected purlin flange
x_2	depth of purlin web included in beam-column section to obtain correct stress distribution in unconnected purlin flange
x_A, y_A, θ_{AB}	displacements and rotation in local x-y axes
y	distance from centroid of effective purlin section to extreme outer flange fibre
	or midspan deflection of simply-supported beam
y_H	midspan deflection of simply-supported beam
α	distance from centre of purlin rotation to the flange-web junction divided by H
λ	load factor
σ_x	in-plane bending stress
σ_y	out-of-plane bending stress
$[g_m]$	geometric element stiffness matrix
$[G]$	geometric global stiffness matrix
$[k_m]$	linear elastic element stiffness matrix
$[k_m^*]$	second order element stiffness matrix
$[K]$	linear elastic global stiffness matrix
$[r_m]$	element restraint matrix
$[R]$	global restraint matrix
$\{F_m\}$	vector of forces in local x-y axes
$\{x_m\}$	vector of joint displacements in local x-y axes
$\{X\}$	vector of joint displacements in global X-Y axes

APPENDIX C. TABLES

(1 kN = 225 lb, 1 N/mm^2 = 145 lb/in.^{2}, 25.4mm = 1 in.)

k (N/mm^2)	P_{cr} (kN)	P_b (kN)	P_{cr}/P_b
0.00	242.19	242.19	1.00
0.01	299.00	291.83	1.03
0.02	335.21	341.49	0.98
0.03	398.07	391.13	1.02
0.04	441.08	440.77	1.00
0.05	480.44	490.43	0.98
0.06	539.51	540.07	1.00
0.07	591.28	589.73	1.00

Table 1: Comparison of Buckling Loads of a Beam with Axial Compressive Loading

k (N/mm^2)	P_{cr} (kN)	P_b (kN)	P_{cr}/P_b
0.00	499.96	499.54	1.00
0.01	573.23	597.09	0.96
0.02	672.74	692.83	0.97
0.03	772.28	786.66	0.98
0.04	882.04	878.61	1.00
0.05	968.75	968.59	1.00
0.06	1051.16	1056.52	0.99
0.07	1144.56	1142.31	1.00

Table 2: Comparison of Buckling Loads of a Beam with Distributed Axial Compressive Loading

k (N/mm^2)	y_H (mm)	y (mm)	y_H/y
0.0001	0.407	0.407	1.00
0.018	0.405	0.406	1.00
0.027	0.403	0.404	1.00
0.055	0.400	0.400	1.00
0.061	0.399	0.399	1.00
0.085	0.396	0.396	1.00
0.090	0.395	0.395	1.00

Table 3: Comparison of Deflections of a Beam with Uniformly Distributed Gravity Loading

k (N/mm^2)	y_H (mm)	y (mm)	y_H/y
0.0001	0.407	0.407	1.00
0.018	0.405	0.405	1.00
0.027	0.404	0.404	1.00
0.055	0.400	0.400	1.00
0.061	0.400	0.399	1.00
0.085	0.397	0.396	1.00
0.090	0.396	0.396	1.00

Table 4: Comparison of Deflections of a Beam with Uniformly Distributed Gravity and Axial Compressive Loading

(i)　　　　　　　　(ii)　　　　　　　　(iii)

Distorted (D) section model

(i)　　　　　　　　(ii)　　　　　　　　(iii)

Undistorted (U) section model
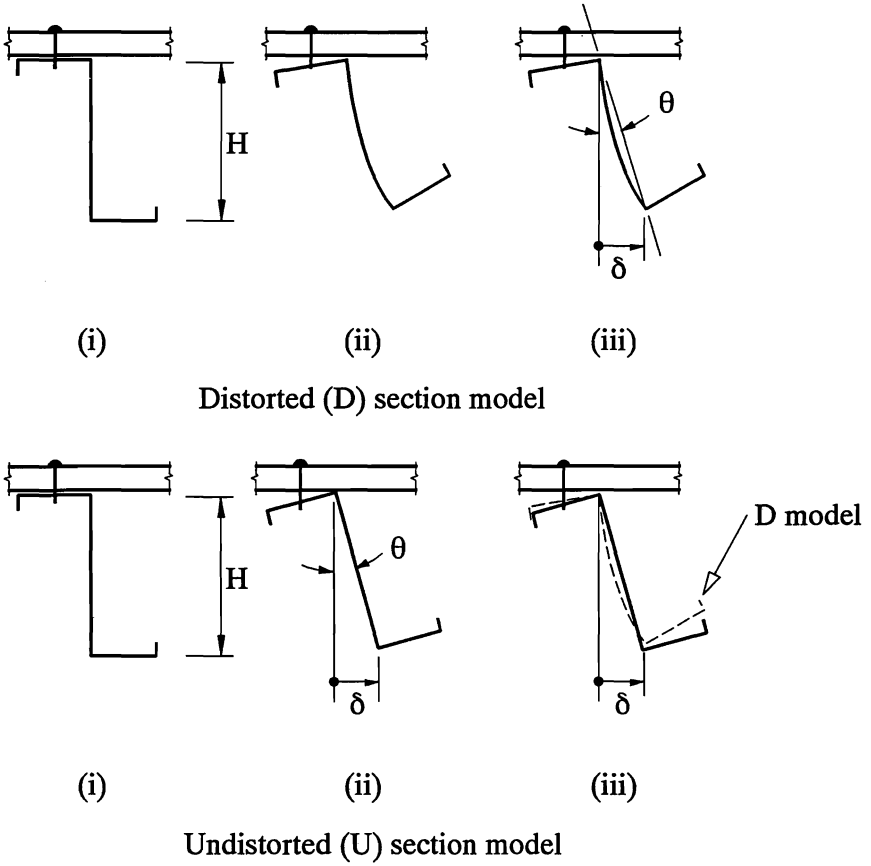
Fig.1(a) D and U Section Models for a Z-section

(i)   (ii)   (iii)

Distorted (D) section model

(i)   (ii)   (iii)   D model

Undistorted (U) section model
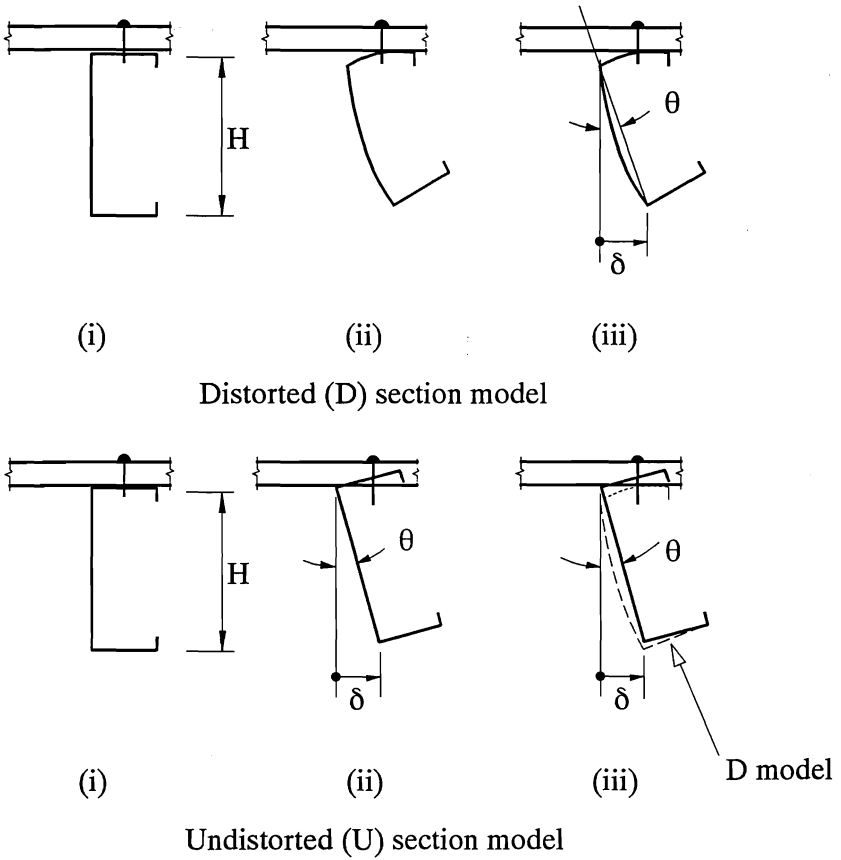
Fig.1(b) D and U Section Models for a Channel

Sheeting

H

b

t

=

Torsion
Stage

+

Vertical Bending
Stage
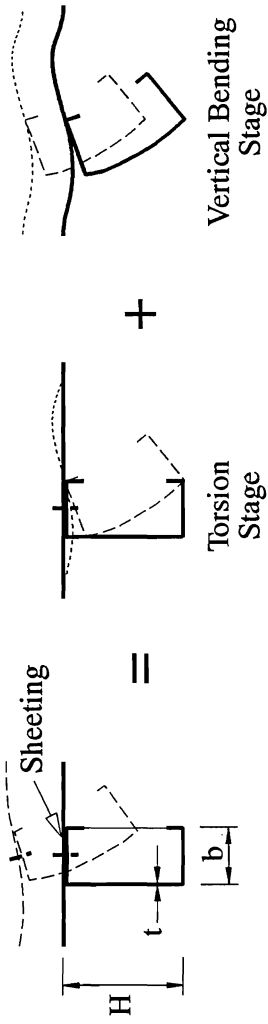
(a) Deformation of a channel

Unconnected
purlin flange

Lateral restraint, k

H

δ

w

+

Conventional
bending theory
with I computed
for twisted section

Torsion Stage

Vertical Bending Stage
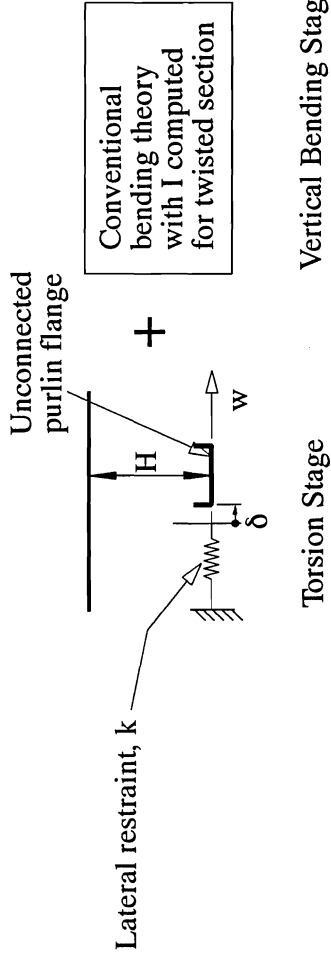
(b) Beam-column model

Fig.2 Peköz and Soroushian Distorted Section Model
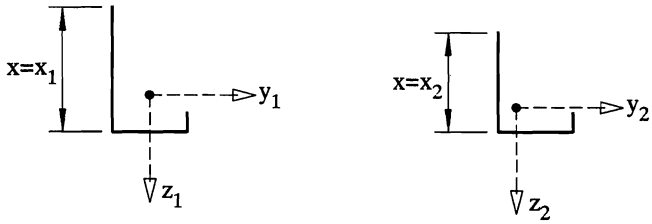
(a) Correct lateral deflections   (b) Correct stress distributions

Fig.3 Thomasson Beam-Column Sections

(a) Typical continuous purlin- sheeting system

(b) Idealised beam-column in second order analysis model
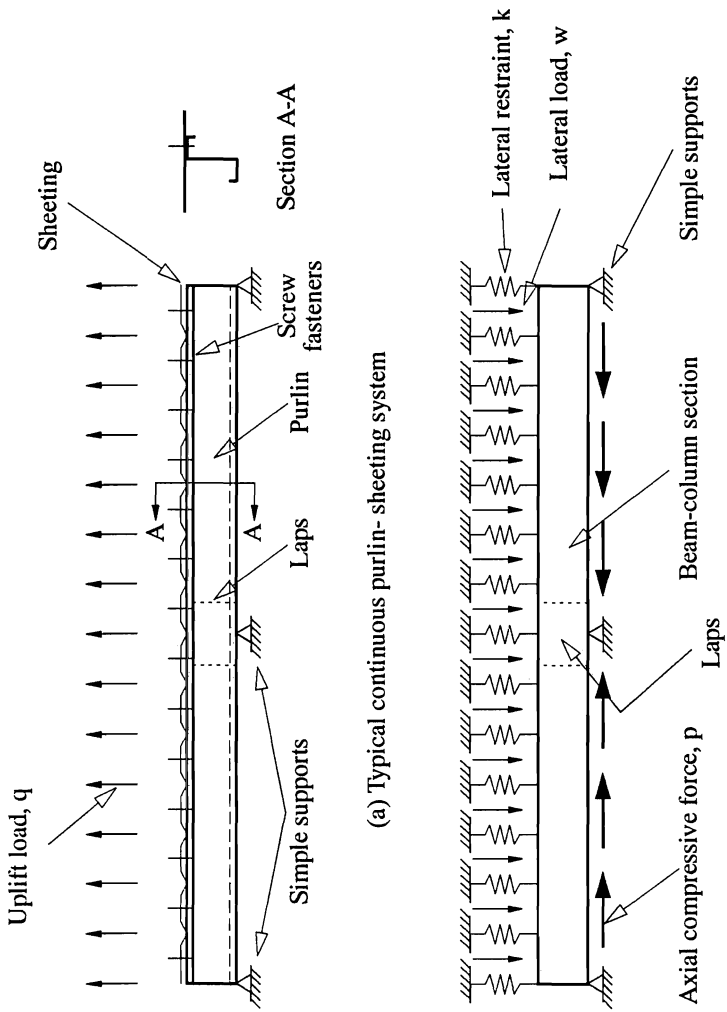
Fig.4 Continuous Purlin Model
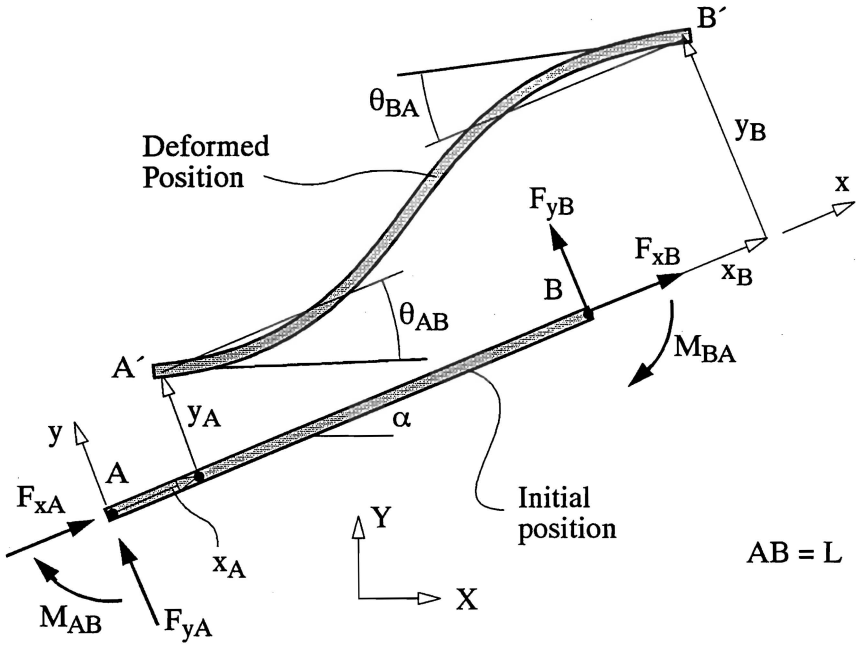
Fig.5 Element Forces and Joint Displacements
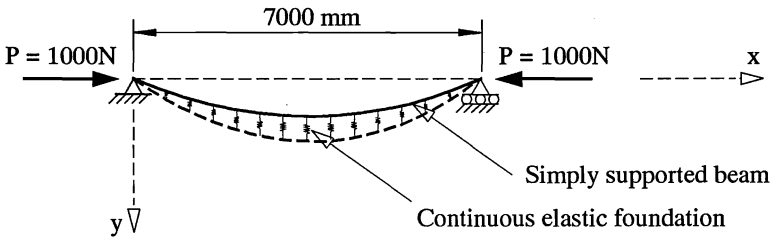
(a) Axial compressive loading
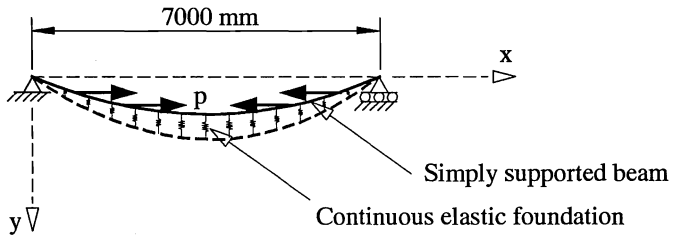
(b) Distributed axial compressive loading

Fig.6 Buckling of a Beam on an Elastic Foundation
(1 N = 0.225 lb., 25.4 mm = 1 in.)
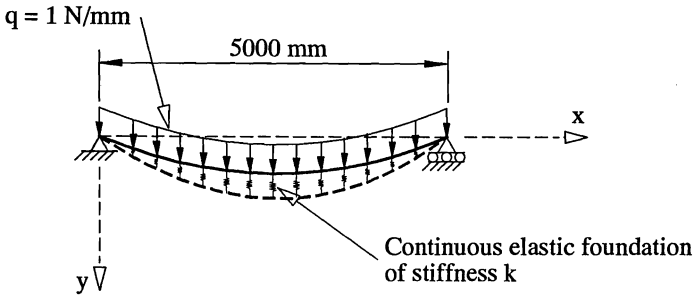
(a) Uniformly distributed loading
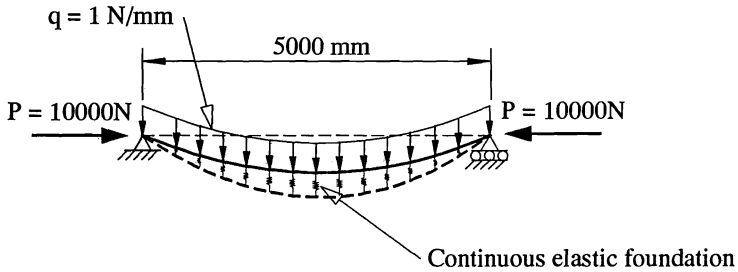
(b) Combined uniformly distributed
and axial compressive loading

Fig.7 Deflection of a Beam on an Elastic Foundation

(1 N = 0.225 lb., 1 N/mm = 5.7 lb/in., 25.4 mm = 1 in.)
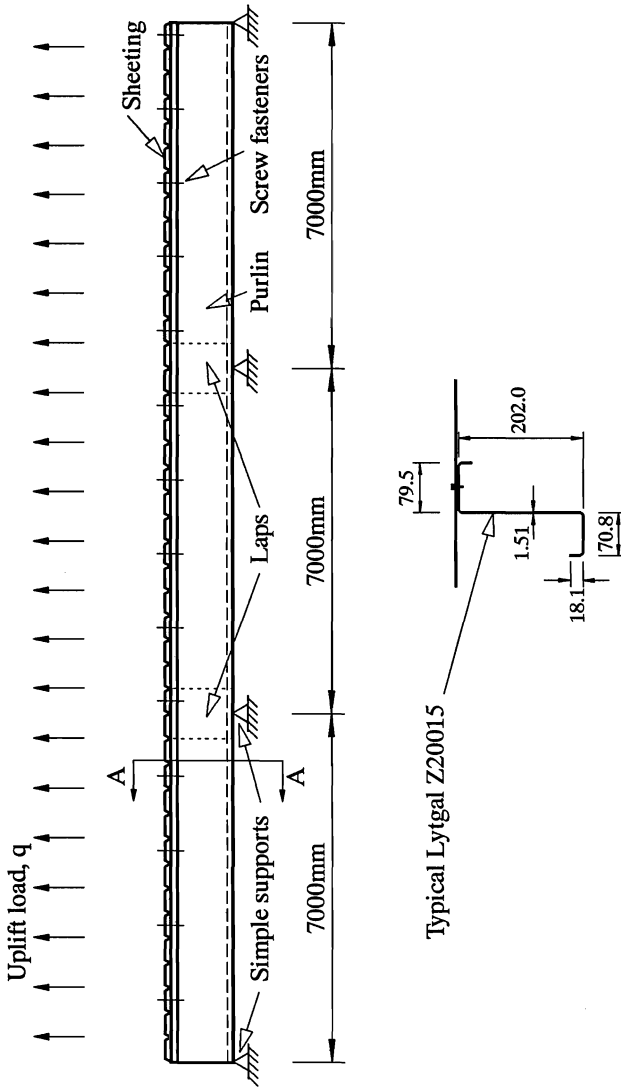
Fig.8 Three Span Continuous Lapped Purlin-Sheeting System under Wind Uplift

(25.4 mm = 1 in.)

144
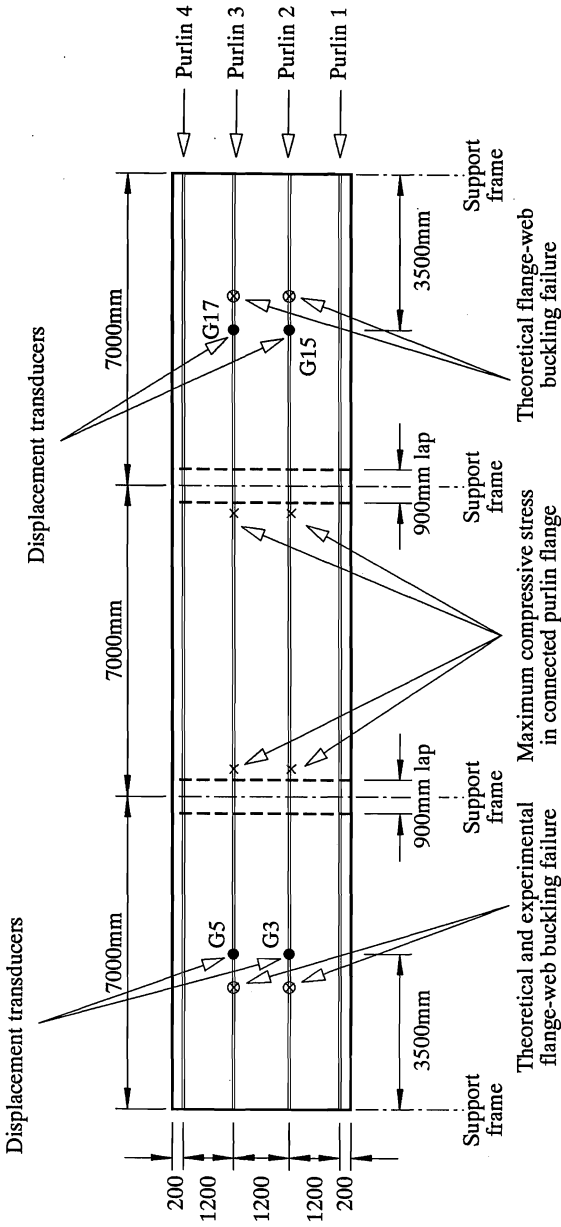
Fig.9 Vacuum Rig Dimensions - Series 1 Test 4(A)

(25.4 mm = 1 in.)
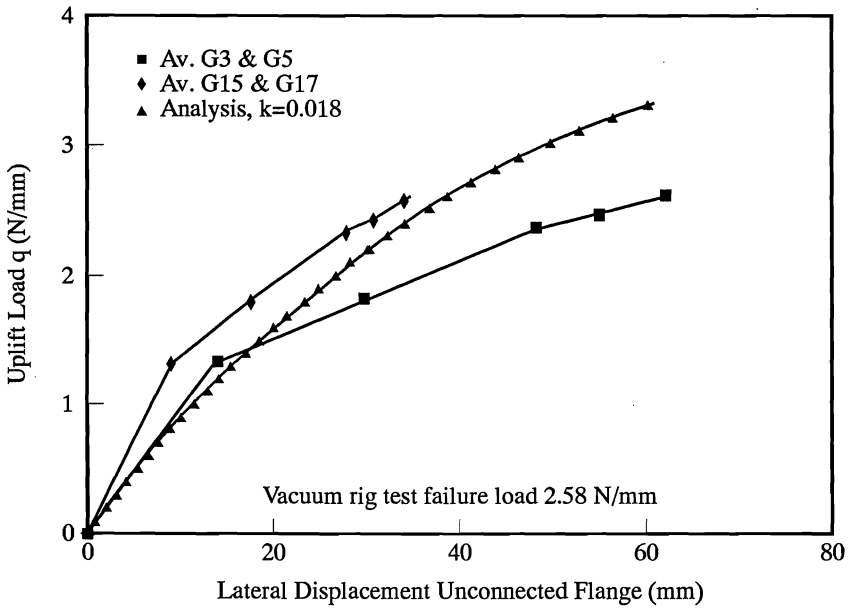
Fig.10 Comparison of Second Order Analysis with
Vacuum Rig Test for Wind Uplift Loading

(1 N/mm = 5.7 lb/in., 25.4 mm = 1 in.)

272 MPa

+ Tension
− Compression

Connected flanges

290 MPa

Flange-web junction

Unconnected flanges

331 MPa

203 MPa

413 MPa

95 MPa

(a) Maximum compressive stress at
flange-web junction, near
midpoint of end spans

(b) Maximum compressive stress in
connected flange, adjacent
to lapped joints
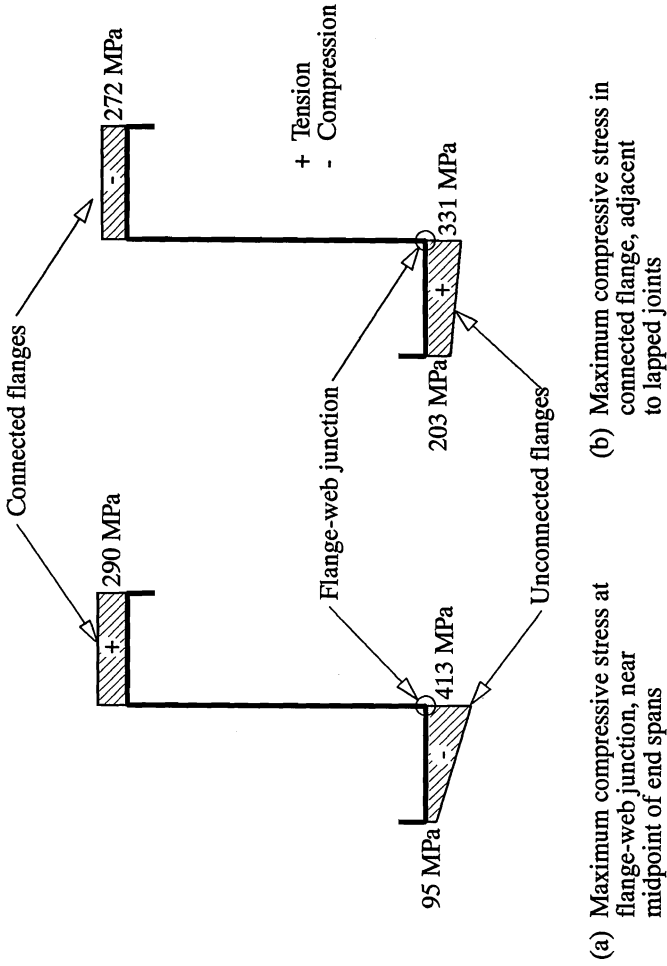
Fig.11 Stress Distributions at Failure for a Z20015 Purlin under Wind Uplift

(6.895 MPa = 1 ksi)

147
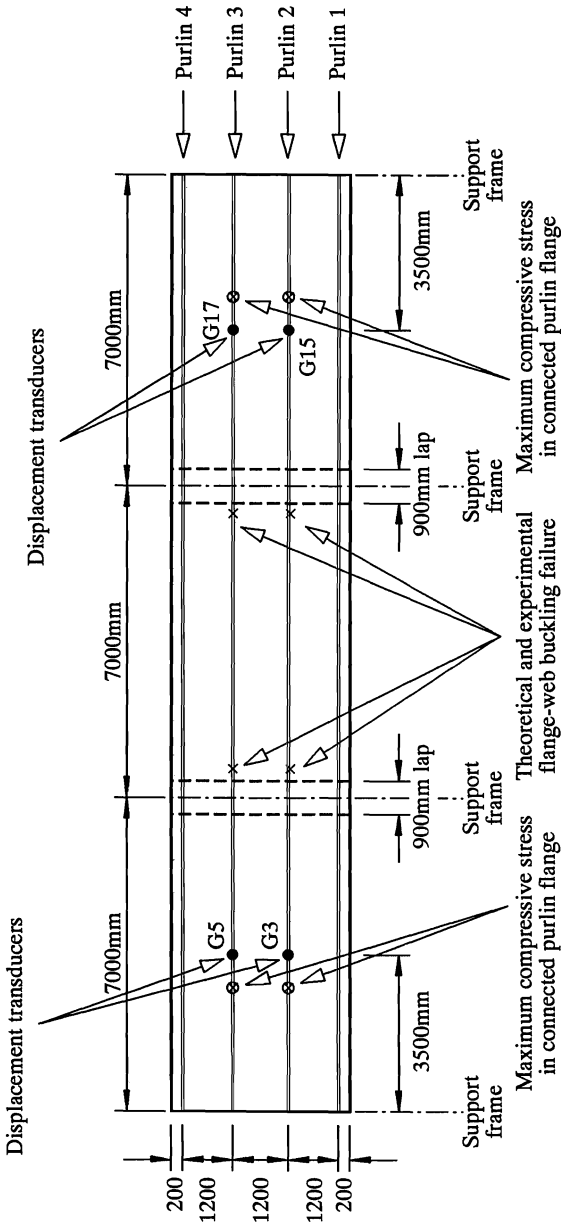
Fig.12 Vacuum Rig Dimensions - Series 4 Test 4

(25.4 mm = 1 in.)
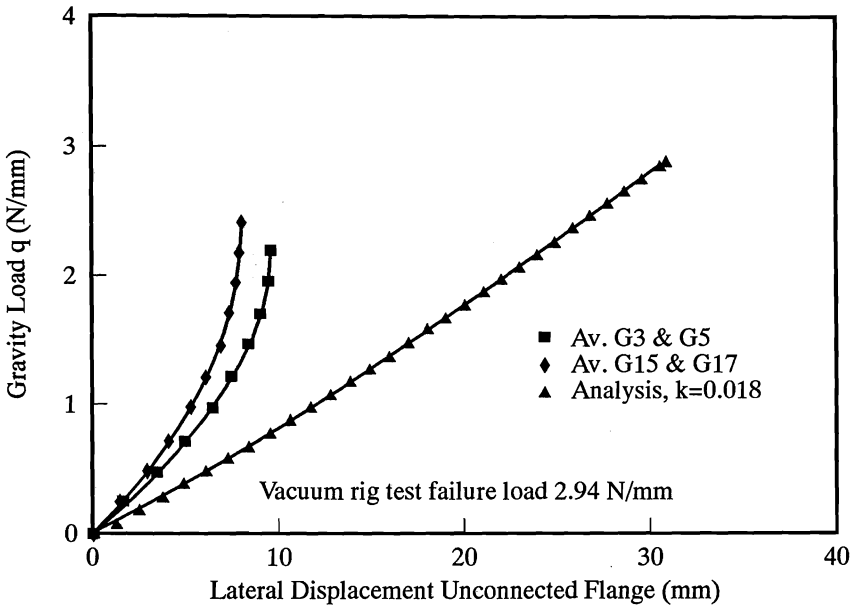
Fig.13 Comparison of Second Order Analysis with
Vacuum Rig Test for Gravity Loading
(1 N/mm = 5.7 lb/in., 25.4 mm = 1 in.)

149

329 MPa

Connected flanges

320 MPa

+

Flange-web junction

437 MPa

−

92 MPa

Unconnected flanges

276 MPa

358 MPa

+

(a) Maximum compressive stress at flange-web junction, adjacent to lapped joints

(b) Maximum compressive stress in connected flange, near midpoint of end spans
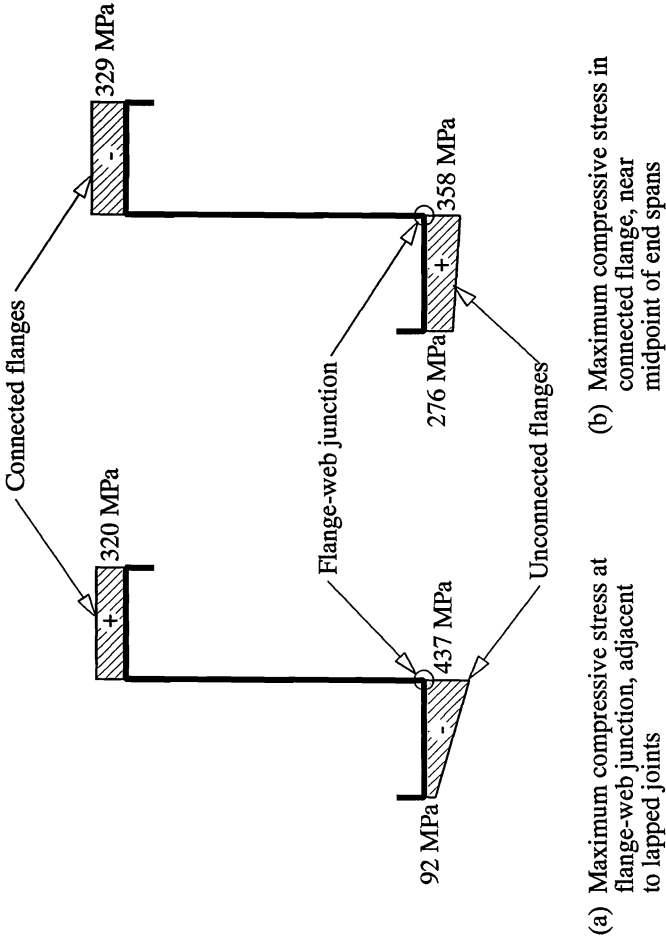
Fig.14 Stress Distributions at Failure for a Z20015 Purlin under Gravity Loading

(6.895 MPa = 1 ksi)